frontiers | Frontiers in Materials

TYPE Original Research
PUBLISHED 17 August 2022
DOI 10.3389/fmats.2022.982861

OPEN ACCESS

EDITED BY
Grzegorz Golewski,
Lublin University of Technology, Poland

REVIEWED BY
Asad Hanif,
King Fahd University of Petroleum and Minerals, Saudi Arabia
Shengwen Tang,
Wuhan University, China

*CORRESPONDENCE
Yanxin Chen,
chenyanxin@xauat.edu.cn

SPECIALTY SECTION
This article was submitted to Structural Materials,
a section of the journal
Frontiers in Materials

RECEIVED 30 June 2022
ACCEPTED 15 July 2022
PUBLISHED 17 August 2022

CITATION
Jiu S, Wang M, Chen Y, Chen J and Gao Q (2022), Synthesis and characterization of low-carbon cementitious materials from suspended calcined coal gangue.
Front. Mater. 9:982861.
doi: 10.3389/fmats.2022.982861

Synthesis and characterization of low-carbon cementitious materials from suspended calcined coal gangue

Shaowu Jiu, Mingming Wang, Yanxin Chen*, Jingyi Chen and Qianwen Gao

School of Materials and Engineering, Xi'an University of Architecture and Technology, Xi'an, China

Coal gangue is used to replace cement clinker to prepare cementitious material *via* activation techniques. Thus, the solid waste can be effectively disposed, and the carbon emission from cement production processes can be significantly reduced. In this paper, the product transformation, reaction mechanism, and thermal activation kinetics of coal gangue were analyzed by X-ray diffraction, thermal analysis, infrared analysis, and scanning electron microscopy. We employed a suspension calcination process to prepare high-activity metakaolin. A cementitious material was prepared from the metakaolin and cement, and the mechanical properties and hydration products were analyzed. The results show that metakaolin was formed by the dehydroxylation of kaolinite in the coal gangue during calcination, and the reaction was based on the *Z–L–T* three-dimensional diffusion mechanism with an activation energy of 190.2 kJ/mol. Metakaolin with dissolution rates of 69.5%–76.3% and 44.5%–52.3% of activated alumina and silica, respectively, were synthesized by calcining the coal gangue at 750°C–850°C for approximately 5 s *via* suspension calcination. The prepared cementitious material showed 28-days compressive strength of 57.5–61.5 MPa and an activity index of 114%–135%. The cementitious material participated in the hydration of cement and formed a structurally dense hardened body, which resulted in a high replacement volume and high strength of the specimens. The preparation of low-carbon cementitious materials by activating gangue *via* suspension calcination provides a basis for gangue utilization and reduction of carbon emissions during cement production.

KEYWORDS

coal gangue, reaction mechanism, suspension calcination, cementitious materials, compressive strength

1 Introduction

Globally, coal gangue is mainly disposed of in landfills due to the lack of effective utilization technology. It not only occupies a large amount of land but also causes severe environmental pollution (Yu et al., 2012; Zhang et al., 2015; Gao et al., 2021). Metakaolin can be prepared by calcining coal gangue with kaolinite as the main component and is used as an auxiliary cementitious material in cement production to replace a portion of cement clinker, thereby reducing the amount of cement in concrete and significantly improving its durability and late strength (Lee et al., 2005; Li et al., 2006; Cassagnabère et al., 2010; Shekarchi et al., 2010). Therefore, the use of coal gangue for cement production has the dual effect of utilizing coal gangue and reducing carbon emissions in the cement industry (Tironi et al., 2012; Cheng et al., 2021; Guan et al., 2021).

Currently, gangue is mainly used as a blend, in which it is only less than 15%–20%, which limits its utilization (Dhandapani et al., 2018; Zhang et al., 2021; Zhao et al., 2021). Karen and Dhandapani (Dhandapani et al., 2018; Scrivener et al., 2018) reported that blends of calcined clay and limestone powder could be significantly increased to 45% in cement, and performance comparable to that of pure silicate cement is achieved. Kaolinite, as the main constituent of the gangue, is also a clay. Therefore, it is theoretically feasible to use calcined gangue instead of clay to prepare cementitious materials. Liu et al. (2021) substituted calcined gangue and limestone powder for cement and achieved a maximum admixture of 30%, which confirmed that the use of activated gangue for Karen and Dhandapani cementitious material systems was also feasible in practice. A muffle furnace was usually used for calcining gangue, and a rotary kiln calcination system was mainly used in practice. Gangue is mainly calcined in a stacked state, which takes 2–6 h to form activity; thus, it consumes high energy and yields unstable product quality (Alireza et al., 2015; Liu et al., 2017; Sun et al., 2019). Suspension calcination was a new technique for gangue calcination. Powder with particle sizes of 100 μM or less is used as a raw material and is carried by a conveying bed, which significantly reduces the calcination time and energy consumption and effectively prevents the unstable activity caused by uneven calcination degree (Bich et al., 2009; Diffo et al., 2015; Jiu et al., 2021). However, suspension calcination of gangue has not been extensively studied, either experimentally or theoretically (Frías et al., 2012; Liu et al., 2017).

In this study, the physical properties, calcination reaction kinetics, and suspension calcination of coal gangue were investigated using low-quality coal gangue as the raw material. The activated gangue products calcined *via* suspension were used to prepare a low-carbon cementitious material, and the mechanical properties and microstructure after hydration were studied. The carbon emission reduction effect of the materials was also analyzed.

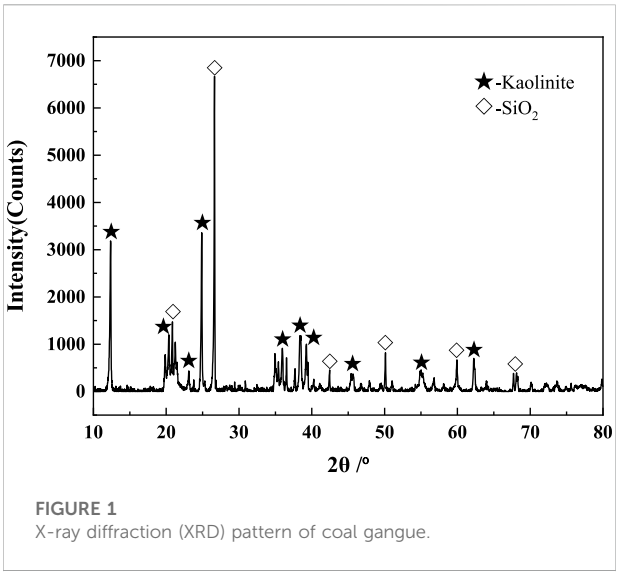

FIGURE 1
X-ray diffraction (XRD) pattern of coal gangue.

2 Experimental

2.1 Raw materials

The raw material was high-alumina-type gangue from Fushun, Liaoning Province, China. The gangue was crushed to a particle size of less than 5 mm using a jaw crusher and dried in an oven at 105°C ± 0.5°C. The dried granular material was ground into a fine powder with particle sizes less than 80 μM (d50 = 15.82 μM) using a sample-making machine. The mineral composition of the materials was analyzed by X-ray diffraction (XRD; D/MAX-2200, Rigaku, Japan) using a Cu Kα target at tube voltage and current of 45 kV and 40 mA, respectively. The XRD patterns of the raw materials are shown in Figure 1.

The chemical composition of the gangue was analyzed by X-ray fluorescence spectrometry (XRF; S4PIONEER, Bruker, Germany). The X-ray tube was operated at a power of 4.2 kW and maximum voltage and current of 60 kV and 140 mA, respectively. The XRF results are listed in Table 1.

TABLE 1 Elemental analysis of coal gangue (wt%).

SiO_2	Al_2O_3	Fe_2O_3	K_2O	TiO_2	MgO	Na_2O	SO_3	CaO	Cl	P_2O_5	ZrO_2
56.38	24.37	1.87	1.23	1.29	0.78	0.14	0.048	0.165	0.06	0.12	0.125

TABLE 2 Common $G(\alpha)$ functions for solid-state reactions.

Symbol of $G(\alpha)$	Sequence number of functions	Equation name	Expression of $G(\alpha)$ function
D1	1	One-dimensional diffusion	α^2
D2	2	Two-dimensional diffusion	$\alpha + (1-\alpha)\ln(1-\alpha)$
1D3	6	Three-dimensional diffusion (spherically symmetric)	$[1-(1-\alpha)^{1/3}]^2$
2D3	9	Three-dimensional diffusion	$[1-(1-\alpha)^{-1/3}]^2$
A1	16	Nucleation and growth (n = 1)	$-\ln(1-\alpha)$
A2/3	17	Nucleation and growth (n = 3/2)	$[-\ln(1-\alpha)]^{3/2}$
A2	13	Nucleation and growth (n = 1/2)	$[-\ln(1-\alpha)]^{1/2}$
A3	11	Nucleation and growth (n = 1/3)	$[-\ln(1-\alpha)]^{1/3}$
R2	31	Shrinking core (cylindrically symmetric)	$1-(1-\alpha)^{1/2}$
R3	29	Shrinking core (spherically symmetric)	$1-(1-\alpha)^{1/3}$
P2	24	Power law	$\alpha^{1/2}$
P3	23	Power law	$\alpha^{1/3}$
C2	37	Chemical reaction	$(1-\alpha)^{-1}-1$
C1.5	38	Chemical reaction	$(1-\alpha)^{-1/2}$

XRD and XRF analyses revealed that the kaolinite and quartz contents of the gangue were approximately 64.10 wt% and 28.82 wt%, respectively; thus, it was a low-grade gangue.

2.2 Kinetic analysis

A coupled system of NETZSCH Model 409PC TGA-DSC simultaneous thermal analyzer and Bruker FTIR-7600 infrared spectrometer was used for the kinetic analysis. The test conditions were as follows: air atmosphere with a flow rate of 80 ml/min, temperature ramping rates of 10°C/min, 20°C/min, 30°C/min, and 40°C/min, and a sample volume of 6.5 ± 0.5 mg. The wave number range for the infrared analysis spectrum of the escaping gas was 4000–600 cm^{-1}.

The kinetics were calculated based on the thermogravimetry (TG) data. The temperature range of $H_2O_{(g)}$ release was first detected by Fourier transform infrared (FTIR) spectroscopy, and the corresponding TG data in this temperature range were obtained to calculate the reaction conversion α using the following equation (Yang and Hu, 1986; Vyazovkin and Wight, 1998):

$$\alpha = (m_0 - m_i)/(m_0 - m_\infty) \quad (1)$$

where m_0 is the mass of the sample at the beginning of the reaction (%), m_∞ the mass at the end of the reaction (%), and m_i the mass at a moment during the reaction (%).

The integral form of the kinetic equation for the solid-phase reaction is as follows (Yang et al., 1986; Vyazovkin and Wight, 1998):

$$G(\alpha) = A\,exp(-E/RT)\cdot t \quad (2)$$

where E is the activation energy of the reaction (kJ/mol), A is the prefactor (s^{-1}), and G(α) is the integral form of the mechanism function. The commonly used G(α) functions for solid-phase reactions are listed in Table 2 (Hu and Shi, 2001). The kinetics analysis was conducted to determine E, A, and $G(\alpha)$.

The kinetics of the reaction were calculated from α–T plot using the Kissinger and general integration methods (Juan et al., 1992; Blaine and Kissinger, 2012). The Kissinger method was expressed as follows (Blaine and Kissinger, 2012):

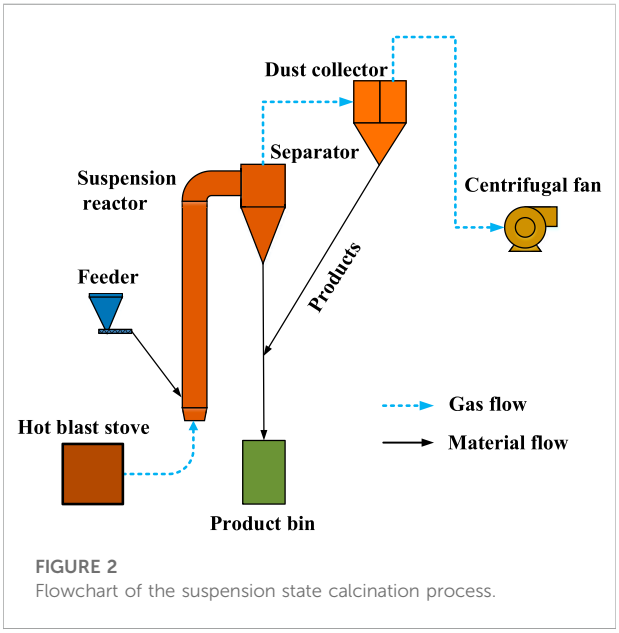

FIGURE 2
Flowchart of the suspension state calcination process.

TABLE 3 Mixing proportion of pastes.

Sample	Cement (g)	Calcined coal gangue (g)	Limestone powder (g)	Water (g)
P	360	0	0	144
A1	252	54	54	
A2		72	36	
A3		81	27	
B1	216	72	72	
B2		96	48	
B3		108	36	
C1	180	90	90	
C2		120	60	
C3		135	45	

$$ln\left(\frac{\beta_i}{T_{pi}^2}\right) = ln\frac{AR}{E} - \frac{E}{R}\frac{1}{T_{pi}},\ i = 1, 2, 3, 4 \quad (3)$$

where β_i is the rate of temperature rise (°C/min), and T_{pi} is the peak temperature on the differential thermogravimetry (DTG) curve (K). The general integral is expressed as follows (Juan et al., 1992):

$$ln\left[\frac{G(\alpha)}{T^2}\right] = ln\left\{\frac{AR}{\beta E}\left(1 - \frac{2RT}{E}\right)\right\} - \frac{E}{RT} \quad (4)$$

For a chosen $G(\alpha)$, if the fitted curve of experimental data according to ln $[G(\alpha)/T^2]$ − 1/T was linear, $G(\alpha)$ was the correct mechanism function. E and A can be obtained from the slope and intercept of the line, respectively. Substituting E, A, and $G(\alpha)$ into Eq. 2, we obtained the equations for the gangue dehydroxylation reaction kinetics. The temperature and time for the suspension calcination could be determined by the kinetics equations.

2.3 Suspension state calcination system

The system of calcining coal gangue in the suspension state is shown in Figure 2. The system consists of a hot blast stove, feeder, suspension reactor, separator, dust collector, product bin, centrifugal fan, etc. The hot blast stove used kerosene as fuel. The feeder consists of a silo and a screw conveyor. The suspension reactor was a tubular furnace made of heat-resistant stainless steel. The exterior of the furnace was covered with a compensating electric heating sleeve to keep the temperature stable. The separator was a cyclone, which collects the material after calcination. The dust collector was a

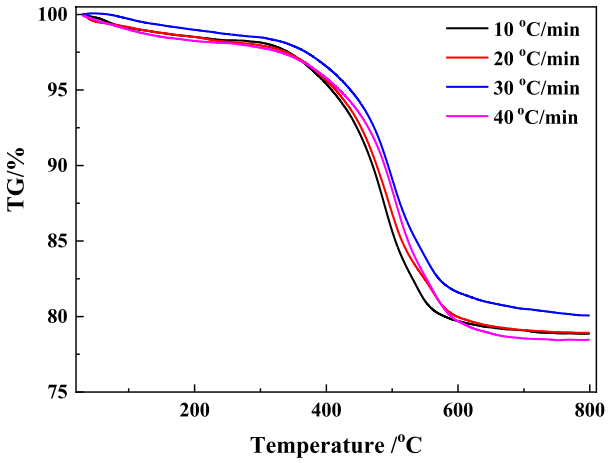

FIGURE 3
Thermogravimetry analysis (TGA) patterns of the coal gangue.

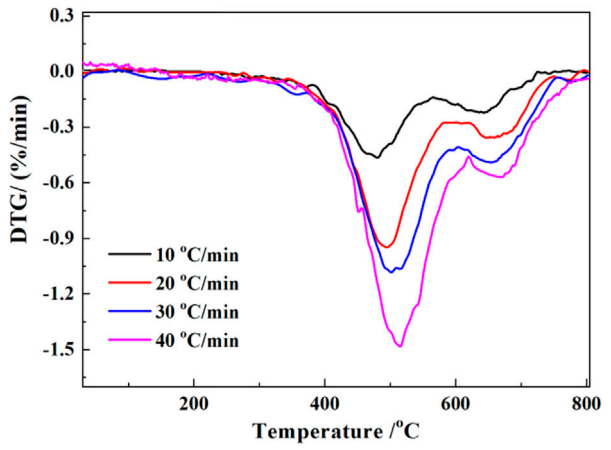

FIGURE 4
Differential thermogravimetry (DTG) mapping of the coal gangue.

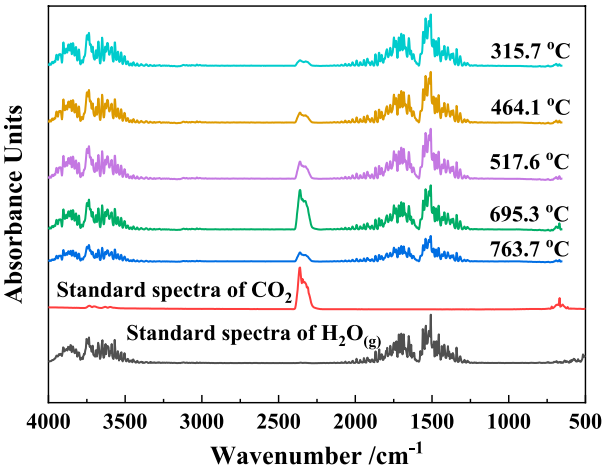

FIGURE 5
Two-dimensional Fourier transform infrared (FTIR) spectra of the gas products.

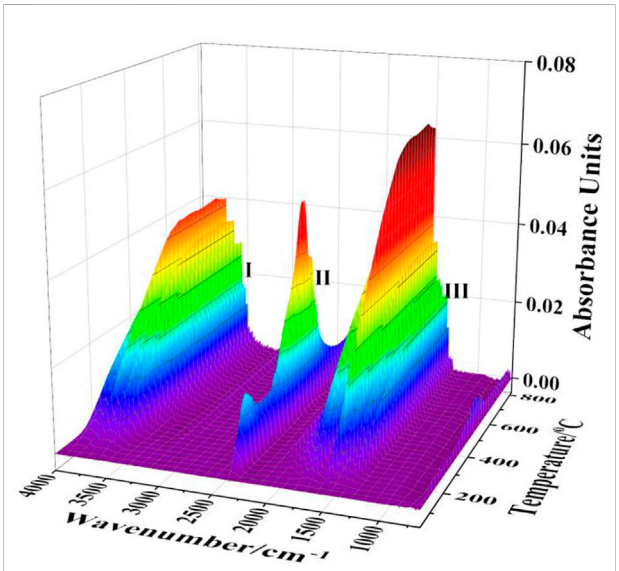

FIGURE 6
Three-dimensional (FTIR) spectra of the gas products.

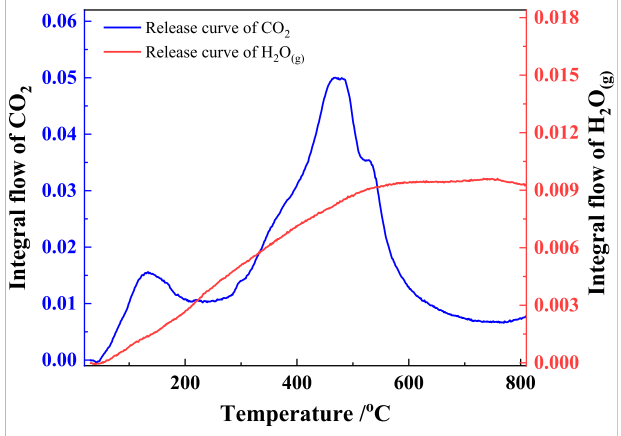

FIGURE 7
Release flow of gas products.

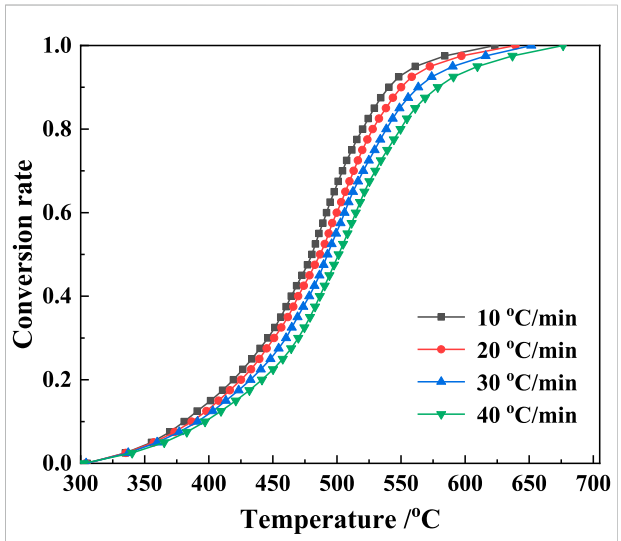

FIGURE 8
Conversion rates of the gangue at different heating rates.

bag-type structure, which collects the fine material that cannot be collected by the cyclone. The product bin was a closed cylinder, which collects the calcined gangue product discharged from the separator and dust collector. The system was negative pressure and powered by a centrifugal fan.

The calcination was conducted in a temperature range of 750°C–850°C, a residence time of approximately 5 s, and a charge rate of 15 ± 0.5 kg/h. The activity of the calcined products in the suspension state was characterized by XRD, and the dissolution rates of activated alumina and silica were determined by potassium fluorosilicate volumetry and spectrophotometry, respectively (Qiu and Pang, 1989; Zhen et al., 2007).

2.4 Performance analysis of the cementitious materials

Thecalcined gangue, limestone powder, and reference cement were mixed in certain ratios to prepare cementitious materials. Samples with calcined-gangue–limestone-powder ratios of 1:1, 2:1, and 3:1 were prepared to conduct 10 sets of tests (including the control sample test) at three cement blending levels of 50%, 60%, and 70%. The dosing schemes are listed in Table 3.

TABLE 4 Reaction kinetics fitting results.

Method	*B* (°C/min)	*E* (kJ/mol)	*A*	*r*
General integral method	10	191.81	6.93×10^{11}	0.991813
	20	189.46	6.96×10^{11}	0.993607
	30	189.60	7.63×10^{11}	0.995097
	40	189.91	7.22×10^{11}	0.995672
Kissinger method	——	184.56	——	0.983538

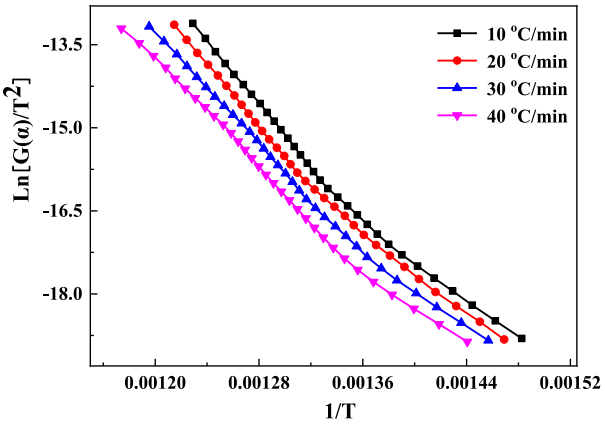

FIGURE 9
Fitting curves for mechanism function No. 9, based on the general integration method.

The compressive strengths of the block samples were measured on 3, 7, and 28 days according to the GB/T 17671 "Test method of cement sand strength." Cement specimens were prepared with a fixed water–cement ratio of 0.4, placed in a standard conditioning chamber at 20°C and 90% air humidity, and conditioned by extracting fragments from the middle of the specimen and soaking in anhydrous ethanol for 48 h to terminate hydration at 3, 7, and 28 days to determine the strength. The specimens were removed, dried in a vacuum oven for 8 h, and then placed in sealed bags for SEM–energy dispersive spectroscopy analyses.

3 Results and discussion

3.1 Thermal analysis of raw materials

The TG and DTG results of the coal gangue are shown in Figures 3, 4, respectively. There were three major stages of mass loss during the calcination process of coal gangue (Figure 3). The first stage occurred before 200°C with a mass change rate of 1.25%–1.93%. The second stage occurred at 280°C–605°C, which was the major stage of the reaction with a mass change rate of 18.72%–19.73%. The third stage occurred at 605°C–795°C, and the mass change rate was 1.62%–1.83%. The two peaks of the second and third phases partially overlap (Figure 4), indicating a crossover temperature range between these two phases of the reaction.

The two-dimensional infrared absorption spectra of the gangue at different temperatures are shown in Figure 5. The gas products released during the gangue calcination process included mainly two functional groups, carbonyl and hydroxyl groups, which correspond to CO_2 and $H_2O_{(g)}$, respectively (Carlos et al., 2009; Hamedi and Maham, 2013). $H_2O_{(g)}$ mainly originated from the evaporation of the adsorbed water and the decomposition of kaolinite, and CO_2 was generated from the combustion of coal based on the chemical composition of coal gangue. The three-dimensional infrared absorption spectra of the released gas from the gangue heated at a rate of 20°C/min were shown in Figure 6. Peaks I and III are the infrared absorption peaks of $H_2O_{(g)}$, and peak II corresponds to that of CO_2. The intensity of infrared absorption varied with the amount of gas released, and the trend of the peak corresponds to the reaction trend of the gaseous products.

The release flux curves of $H_2O_{(g)}$ and CO_2 resolved from peaks I and II in Figure 6, respectively, are shown in Figure 7. The release of $H_2O_{(g)}$ at a heating rate of 20°C/min started from approximately 60°C and rapidly increase thereafter, reaching a maximum at approximately 580°C, and started decreasing above 780°C. The released $H_2O_{(g)}$ originated from the evaporation of the adsorbed water and the decomposition of kaolinite. As shown in Figures 4, 7, the adsorbed water evaporated below 200°C, kaolinite decomposed mainly between 280°C and 670°C, and the reaction was completed between 670°C and 800°C. Figure 7 also shows that CO_2 was released in two steps: the first step occurred below 315°C, and the second occurred between 320°C and 740°C. Based on the combustion characteristics of the coal, the first reaction step was attributed to the combustion of volatile fractions of the coal, and the second reaction was attributed to the combustion of fixed carbon in the coal.

TABLE 5 Calcination time for coal gangue, as calculated using the reaction kinetic equation.

Temperature (°C)	750	775	800	825	850
Complete calcination time (s)	14.62	8.58	5.15	3.17	2.00

In Eq. 4, α, which is in the denominator, cannot be 1.0. Herein, set α = 0.9999.

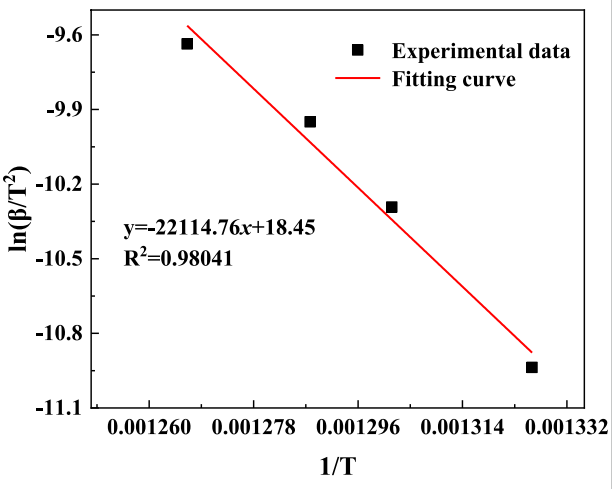

FIGURE 10
Fitting curve based on the Kissinger method.

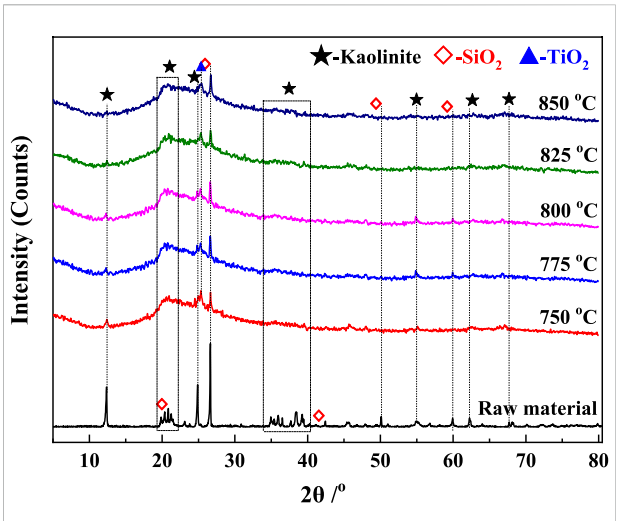

FIGURE 11
XRD patterns of the calcined products in suspension.

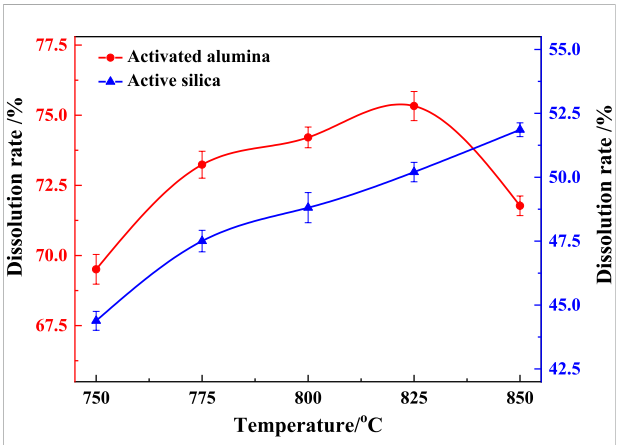

FIGURE 12
Dissolution rates of activated alumina and silica.

3.2 Kinetics of the raw materials

The kaolinite content of the gangue was higher than that of coal, and the mass loss during the calcination was mainly attributed to the decomposition of kaolinite. Therefore, the TG data were appropriate for the kinetic analysis. The TG data were obtained based on Eq. 1, and the conversion rate α curves at four ramp rates were obtained (Figure 8). The Kissinger method was employed to evaluate the reaction kinetics using the DTG peak temperature data. The α–T plot (Figure 8) and the mechanism functions in Table 2 were used to perform a linear fit based on the general integration method. Mechanism function No. 9 showed the highest linearity. The fitting plots based on the general integral and Kissinger methods are shown in Figures 9, 10, respectively.

The fitting results from Figures 9, 10 were listed in Table 4. The linear correlation coefficients of both the Kissinger and general integral methods for the fit of mechanism function No. 9 were greater than 0.98 (Table 4). Meanwhile, the relative deviation of the activation energy obtained from the two methods was only 3.78%, indicating that the kinetic fitting results in Table 4 are reasonable. Mechanism function No. 9 is the Z–L–T diffusion equation, and the decomposition reaction of kaolinite in gangue was controlled by the diffusion rate of $H_2O_{(g)}$ from the reaction interface to the outside of the particles (Tian et al., 2020). The average value of the general integration method was recorded as the final result. The kinetic equation of the coal-based calcination reaction is expressed as follows:

$$\left[(1-\alpha)^{-\frac{1}{3}}-1\right]^2 = 7.19\times10^{11}\, exp\left(-\frac{190.20}{RT}\right).t \qquad (4a)$$

Eq. 4 was used to predict the time required for the complete decomposition of kaolinite in the coal gangue in the temperature range of 750°C–850°C, and the results were listed in Table 5.

Table 5 lists the times required for the complete decomposition of kaolinite to form metakaolinite, as calculated using the reaction kinetic equation with α = 0.9999. Kaolinite can be completely decomposed in less than 25 min to

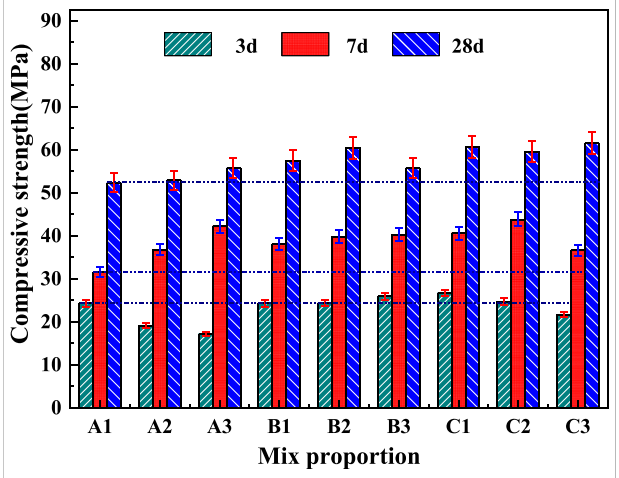

FIGURE 13
Compressive strength of net slurry specimens.

form metakaolin in the temperature range of 750°C–850°C. If α = 0.999, the decomposition time of kaolinite is only 0.58 s, even at 750°C, indicating that kaolinite was decomposed. In practice, under the thermal analysis conditions, the material remains stacked. However, herein, the material was still in a piled state under the thermal analysis conditions. In the suspended state, the powder material was fully dispersed, the transfer conditions were better, and the reaction time was shorter. Thus, the coal gangue was activated in only a few seconds to form metakaolin *via* suspension calcination. The time was considerably reduced compared to the results in the literature (Yuan et al., 2018).

3.3 Characterization of suspended calcined products

3.3.1 XRD analysis

The XRD patterns of the calcined gangue and raw material are compared in Figure 11. The diffraction peaks of kaolinite decreased significantly, almost disappeared after approximately 5 s of calcination in the suspended state, and the XRD patterns of the products show obvious amorphization, indicating that kaolinite was almost completely decomposed to form metakaolinite. For the same calcination time, the diffraction peaks of kaolinite decreased with an increase in temperature, and the diffraction peaks of all kaolinites almost disappeared above 800°C. Compared with the raw materials, the diffraction peaks of SiO_2 in the suspended calcined gangue are significantly stronger. Since the metakaolinite formed by kaolinite decomposition had an indeterminate structure without prominent peaks, the diffraction peaks of quartz in the raw material were highlighted in contrast (Xu et al., 2015). The diffraction peak of TiO_2 appeared at 2θ = 25°, and its content in the raw material could not be detected by XRD. After calcination, TiO_2 was detected due to the unbroken lattice (Hanif et al., 2017). Kaolinite in the coal gangue was completely decomposed to metakaolin when the gangue was calcined at 750°C–850°C for approximately 5 s, which verified that the kinetic model is reliable.

3.3.2 Dissolution rate analysis

The dissolution rates of activated alumina and silica in the calcined gangue were shown in Figure 12. Kaolinite in the gangue formed metakaolin after calcination, and the gelling activity is attributed to the amorphous structure of metakaolin. The higher the dissolution rates of activated alumina and silica were, the higher the gelling activity was. The dissolution rate of activated alumina in calcined gangue ranged from 69.5% to 76.3%, and that of activated silica ranged from 44.5% to 52.3%, indicating that the calcined gangue exhibited a good gelling activity. With the same residence time dung the suspension calcination, the dissolution rate of activated aluminum increased as the calcination temperature increased from 750°C to 825°C, above which it decreased. Therefore, the calcination product at 825°C had the highest activity.

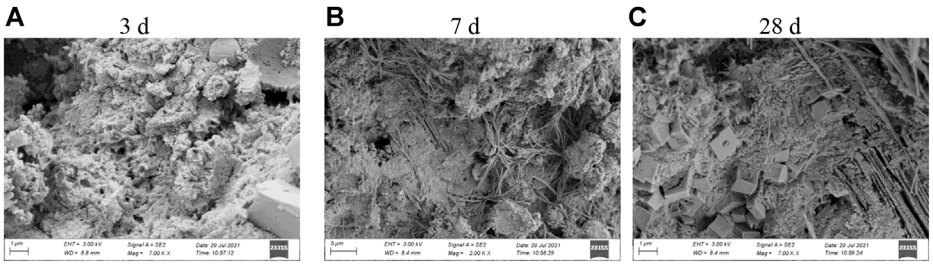

FIGURE 14
SEM images of the net slurry specimen.

3.4 Performance of cementitious materials

3.4.1 Compressive strength

Gelling performance tests were performed using the activated gangue products obtained from the suspension calcination at 825°C for 5 s. The compressive strengths of the net slurry specimens with the ratios in Table 3 at 3, 7, and 28 days are shown in Figure 13. The 3-days compressive strength of the test blocks with different ratios of calcined gangue and limestone was small compared with that of pure cement because metakaolin did not participate in the hydration at the early stage. As the partial kaolin began to hydrate, the compressive strength of the specimens increased, becoming equal to or greater than that of the pure cement at 7 days. The compressive strength of only sample A1 was lower than that of the pure cement. In the late stage of hydration, the admixture fully participated in the hydration to form hardened products. The 28-days compressive strength of the specimens was increased by 14%–35% compared with that of the pure cement specimens, indicating that the gangue calcined exhibited good cementing activity. Compared with the pure cement samples, B1, B2, B3, C1, and C2 showed lower compressive strength at 3 days but higher values at 7 and 28 days. Thus, the C1 scheme was optimal. The percentages of cement replacement in the B and C samples were 40% and 50%, respectively, and the activated gangue was between 20% and 37.0%. Therefore, the gangue calcined at 825°C for 5 s had a cementitious activity index of 114%–135%. It could replace 40%–50% of cement in the range of 20%–37% of admixture, and the 28-days compressive strength of the prepared cementitious material reached 57.5–61.5 MPa.

3.4.2 SEM analysis of the hydrated products

SEM images of the hydrated gelatinized material (sample C1) are shown in Figure 14. The test sample of the cementitious material exhibited a gel structure with numerous pores, and no obvious hydrated minerals were formed (Figure 14A). As hydration proceeded, several hydrated mineral crystals with a fibrous structure embedded in the gel were formed (Figure 14B), and the structure of the specimen became dense. In addition to the fibrous minerals, several hardened regular shapes with dense structures were formed (Figure 14C). Thus, the compressive strength of the cementitious material prepared from the calcined gangue increased compared with that of pure cement, consistent with the study in the literature (Liu and Yan, 2008; Wang et al., 2018; Yang et al., 2022).

3.5 Carbon reduction

Each ton of cement clinker produced consumes approximately 100 kg of standard coal and emits approximately 1 ton of CO_2 based on the current technological status of the cement industry. However, 1 ton of calcined gangue produced by suspension calcination consumes 10–15 kg of standard coal, and the production process emits 37–55 kg of CO_2. The coal consumption is 45–55 kg of standard coal per ton of gelling material, and the CO_2 emission is 420–520 kg, as estimated from the ratios of the B and C samples in Table 3. Approximately 80 kg of standard coal is consumed to produce 1 ton of cement, and 800 kg of CO_2 is emitted based on 15% of blends in ordinary silicate cement. Compared with ordinary Portland cement, the cementitious material prepared with the coal gangue calcined *via* suspension calcination can reduce coal consumption by 30%–43% and CO_2 emission by 35%–47% per ton of cement produced.

4 Conclusion

(1) Kaolinite in the gangue decomposed during calcination to form metakaolin. The reaction was based on a diffusion-controlled mechanism, and the activation energy was 190.2 kJ/mol. The calcination parameters predicted from the kinetic equation were consistent with the actual values.

(2) Products with metakaolin as the major constituent could be obtained by calcining the gangue at 750°C–850°C for approximately 5 s *via* the suspension calcination process. The dissolution rates of activated alumina and silica were 69.5%–76.3% and 44.5%–52.3%, respectively.

(3) The activated coal gangue prepared *via* suspension calcination could replace 40%–50% of cement in the range of 20%–37%. The 28-days compressive strength of the prepared cementitious material was 57.5–61.5 MPa, and the activity index was as high as 114%–135%.

(4) The suspension calcination process is feasible for activating coal gangue, and the prepared cementitious material has significant energy-saving and carbon-reducing benefits.

Data availability statement

The raw data supporting the conclusions of this article will be made available by the authors, without undue reservation.

Author contributions

YC contributed to the conception of the study. SJ performed the experiments, data analyses and wrote the manuscript. MW contributed significantly to analysis and manuscript preparation. JC and QG contributed to

experiments. All authors have read and agreed to the published version of the manuscript.

Funding

This research was funded by Anhui Provincial Science and Technology Major Project (Grant No. 2021e03020003) in China.

Acknowledgments

Author SJ would like to thank Chang Chen for his help in the submission process of this paper.

Conflict of interest

The authors declare that the research was conducted in the absence of any commercial or financial relationships that could be construed as a potential conflict of interest.

Publisher's note

All claims expressed in this article are solely those of the authors and do not necessarily represent those of their affiliated organizations, or those of the publisher, the editors and the reviewers. Any product that may be evaluated in this article, or claim that may be made by its manufacturer, is not guaranteed or endorsed by the publisher.

References

Alireza, S., Farhad, G., and Rahim, N. (2015). An investigation on pozzolanic activity of Iranian kaolins obtained by thermal treatment [J]. *Appl. Clay Sci.* 103, 34–39.

Bich, C., Ambroise, J., and Péra, J. (2009). Influence of degree of dehydroxylation on the pozzolanic activity of metakaolin. *Appl. Clay Sci.* 44, 194–200. doi:10.1016/j.clay.2009.01.014

Blaine, R., and Kissinger, H. (2012). Homer kissinger and the kissinger equation. *Thermochim. Acta* 540, 1–6. doi:10.1016/j.tca.2012.04.008

Carlos, R., Encarnacion, R., and Ana, L. (2009). Thermal decomposition of calcite: Mechanisms of formation and textural evolution of CaO nanocrystals [J]. *Am. Mineralogist* 94, 578–593.

Cassagnabère, F., Mouret, M., Escadeillas, G., Broilliard, P., and Bertrand, A. (2010). Metakaolin, a solution for the precast industry to limit the clinker content in concrete: Mechanical aspects. *Constr. Build. Mater.* 24 (7), 1109–1118. doi:10.1016/j.conbuildmat.2009.12.032

Cheng, S., Ge, K., Sun, T., Shui, Z., Chen, X., and Lu, J. X. (2021). Pozzolanic activity of mechanochemically and thermally activated coal-series kaolin in cement-based materials. *Constr. Build. Mater.* 299, 123972. doi:10.1016/j.conbuildmat.2021.123972

Dhandapani, Y., Sakthivel, T., Santhanam, M., Gettu, R., and Pillai, R. G. (2018). Mechanical properties and durability performance of concretes with limestone calcined clay cement (LC3). *Cem. Concr. Res.* 107, 136–151. doi:10.1016/j.cemconres.2018.02.005

Diffo, B., Elimbi, A., and Cyr, M. (2015). Effect of the rate of calcination of kaolin on the properties of metakaolin-based geopolymers [J]. *J. Asian Ceram. Soc.* 3, 130–138.

Frías, M., Villa, R., Rojas, M., Medina, C., and Juan Valdes, A. (2012). Scientific aspects of kaolinite based coal mining wastes in pozzolan/$Ca(OH)_2$ system [J]. *J. Am. Ceram. Soc.* 95, 386–391. doi:10.1111/j.1551-2916.2011.04985.x

Gao, H., Huang, Y., Li, W., Li, J., Ouyang, S., Song, T., et al. (2021). Explanation of heavy metal pollution in coal mines of China from the perspective of coal gangue geochemical characteristics. *Environ. Sci. Pollut. Res.* 28 (46), 65363–65373. doi:10.1007/s11356-021-14766-w

Guan, X., Chen, J., Zhu, M., and Gao, J. (2021). Performance of microwave-activated coal gangue powder as auxiliary cementitious material. *J. Mater. Res. Technol.* 14, 2799–2811. doi:10.1016/j.jmrt.2021.08.106

Hamedi, S., and Maham, Y. (2013). Enhancement of the efficiency of *in situ* combustion technique for heavy-oil recovery by application of nickel ions [J]. *Fuel* 105, 397–407.

Hanif, A., Parthasarathy, P., Ma, H., Fan, T., and Li, Z. (2017). Properties improvement of fly ash cenosphere modified cement pastes using nano silica. *Cem. Concr. Compos.* 81, 35–48. doi:10.1016/j.cemconcomp.2017.04.008

Hu, R., and Shi, Q. (2001). "Thermal analysis kinetics," in *Chinese*. first ed. (Beijing, China: Science Press), 127–154.

Jiu, S., Cheng, S., Li, H., and Wang, L. (2021). Reaction mechanism of metakaolin materials prepared by calcining coal gangue. *Mat. Res. Express* 8, 015508. doi:10.1088/2053-1591/abd907

Juan, J., Francisco, P., and Guillermo, R. (1992). On the integration of kinetic models using a high-order Taylor series method [J]. *J. Chemom.* 6 (5), 231–246.

Lee, S., Moon, H., Hooton, R., and Kim, J. (2005). Effect of solution concentrations and replacement levels of metakaolin on the resistance of mortars exposed to magnesium sulfate solutions. *Cem. Concr. Res.* 35 (7), 1314–1323. doi:10.1016/j.cemconres.2004.10.035

Li, D., Song, X., Gong, C., and Pan, Z. (2006). Research on cementitious behavior and mechanism of pozzolanic cement with coal gangue. *Cem. Concr. Res.* 36 (9), 1752–1759. doi:10.1016/j.cemconres.2004.11.004

Liu, S., and Yan, P. (2008). Hydration properties of limestone powder in complex binding material [J]. *J. Chin. Ceram. Soc.* 36 (10), 1401–1405.

Liu, Y., Lei, S., Lin, M., Li, Y., Ye, Z., and Fan, Y. (2017). Assessment of pozzolanic activity of calcined coal-series kaolin. *Appl. Clay Sci.* 143, 159–167. doi:10.1016/j.clay.2017.03.038

Liu, Y., Ling, T-C., Wang, M., and Wu, Y. Y. (2021). Synergic performance of low-kaolinite calcined coal gangue blended with limestone in cement mortars. *Constr. Build. Mater.* 300, 124012. doi:10.1016/j.conbuildmat.2021.124012

Qiu, G., and Pang, S. (1989). Spectrophotometric determination of activated aluminium in soil using eriochrome cyanine R[J]. *J. Instrum. Analysis* 8 (4), 68–71.

Scrivener, K., Martirena, F., Bishnoi, S., and Maity, S. (2018). Calcined clay limestone cements (LC3). *Cem. Concr. Res.* 114, 49–56. doi:10.1016/j.cemconres.2017.08.017

Shekarchi, M., Bonakdar, A., Bakhshi, M., Mirdamadi, A., and Mobasher, B. (2010). Transport properties in metakaolin blended concrete. *Constr. Build. Mater.* 24 (11), 2217–2223. doi:10.1016/j.conbuildmat.2010.04.035

Sun, T., Ge, K., Wang, G., Geng, H-N., Shui, Z., Cheng, S., et al. (2019). Comparing pozzolanic activity from thermal-activated water-washed and coal-series kaolin in Portland cement mortar. *Constr. Build. Mat.* 227, 117092. doi:10.1016/j.conbuildmat.2019.117092

Tian, L., Gong, A., Wu, X., Li, J., Liu, C., Yu, X., et al. (2020). Non-isothermal kinetic studies of rubidium extraction from muscovite using a chlorination roasting-water leaching process. *Powder Technol.* 373, 362–368. doi:10.1016/j.powtec.2020.06.015

Tironi, A., Trezza, M. A., Scian, A. N., and Irassar, E. F. (2012). Kaolinitic calcined clays: Factors affecting its performance as pozzolans. *Constr. Build. Mater.* 28 (1), 276–281. doi:10.1016/j.conbuildmat.2011.08.064

Vyazovkin, S., and Wight, C. (1998). Isothermal and non-isothermal kinetics of thermally stimulated reactions of solids. *Int. Rev. Phys. Chem.* 3, 407–433. doi:10.1080/014423598230108

Wang, D., Shi, C., Farzadnia, N., Shi, Z., Jia, H., and Ou, Z. (2018). A review on use of limestone powder in cement-based materials: Mechanism, hydration and microstructures. *Constr. Build. Mater.* 181, 659–672. doi:10.1016/j.conbuildmat.2018.06.075

Xu, X., Lao, X., Wu, J., Zhang, Y., and Li, K. (2015). Microstructural evolution, phase transformation, and variations in physical properties of coal series kaolin powder compact during firing. *Appl. Clay Sci.* 115, 76–86. doi:10.1016/j.clay.2015.07.031

Yang, H., Zhang, S., Lei, W., Chen, P., Shao, D., Tang, S., et al. (2022). High-ferrite Portland cement with slag: Hydration, microstructure, and resistance to sulfate attack at elevated temperature. *Cem. Concr. Compos.* 130, 104560. doi:10.1016/j.cemconcomp.2022.104560

Yang, Z., Hu, R., and Liang, Y. (1986). The determination of most probable mechanism function and kinetics parmeters of thermal decomposition of 2, 6-Sinitrophernci by a stngle Non-Isothermal DSC Curve [J]. *Acta Physico-ChimicaSinica* 1, 13–21.

Yang, Z., and Hu, R. (1986). Numerical method for computing kinetics parameters of exothermic decomposition reaction of energetic materials [J]. *Comput. Appl. Chem.* 4, 326–332.

Yu, L. J., Feng, Y. L., and Yan, W. (2012). "The current situation of comprehensive utilization of coal gangue in China," in *Proceedings of the advanced materials research* (Baech, Switzerland: Trans Tech Publ).

Yuan, S., Li, Y., Han, Y., and Gao, P. (2018). Effects of carbonaceous matter additives on kinetics, phase and structure evolution of coal-series kaolin during calcination. *Appl. Clay Sci.* 165, 124–134. doi:10.1016/j.clay.2018.08.003

Zhang, J., Chen, T., and Gao, X. (2021). Incorporation of self-ignited coal gangue in steam cured precast concrete. *J. Clean. Prod.* 292, 126004. doi:10.1016/j.jclepro.2021.126004

Zhang, Y., Ge, X., Liu, L., Wang, X., and Zhang, Z. (2015). Fuel nitrogen conversion and release of nitrogen oxides during coal gangue calcination. *Environ. Sci. Pollut. Res.* 22 (9), 7139–7146. doi:10.1007/s11356-014-3890-8

Zhao, Y., Qiu, J., Ma, Z., and Sun, X. (2021). Eco-friendly treatment of coal gangue for its utilization as supplementary cementitious materials. *J. Clean. Prod.* 285, 124834. doi:10.1016/j.jclepro.2020.124834

Zhen, J., Zhou, T., and Chen, X. (2007). Study on the reactivity and its fast determination method of metakaoline in synthesizing geopolymer [J]. *Bull. Chin. Ceram. Soc.* 26 (5), 887–900.